Reducing expression of dynamin-related protein 1 increases radiation sensitivity of glioblastoma cells

Chiung-Chyi Shen (ccshen61093@gmail.com)
Taichung Veterans General Hospital https://orcid.org/0000-0002-9622-7394
Wen-Yu Cheng
Taichung Veterans General Hospital
Kuan-Chih Chow
National Chung Hsing University
Ming-Tsang Chiao
Taichung Veterans General Hospital
Yi-Chi Yang
Taichung Veterans General Hospital

Research article

Keywords: DRP1; glioblastoma multiforme; radiation resistance; autophagy; DNA repair; nuclear transport

Posted Date: December 11th, 2019

DOI: https://doi.org/10.21203/rs.2.18627/v1

Abstract

Background: Dynamin-related protein 1 (DRP1) is a GTPase involved in mitochondrial fission, mitochondrial protein imports, and drug sensitivity, suggesting an association with cancer progression. This study is to evaluate the prognostic significance of DRP1 in glioblastoma multiforme (GBM). Methods : DRP1 expression was measured by immunohistochemistry and Western blotting. Correlations between DRP1 expression and clinicopathological parameters were by statistical analysis. Differences in survival were compared by a log-rank test. Results : DRP1 expression was detected in 87.2% (41/47) patients with GBM. Patients with higher DRP1 levels had worse survival ($p = 0.0398$). In vitro , silencing of DRP1 reduced cell proliferation, invasive potential, and radiation resistance. The addition of shikonin inhibited DRP1 expression and increased drug uptake. Moreover, shikonin reduced the nuclear entry of DNA repair-associated enzymes and increased radiation sensitivity, suggesting that to reduce DRP1 expression could inhibit DNA repair and increase the radiation sensitivity of GBM cells. Conclusions : Our results indicate that DRP1 overexpression is a prospective radio-resistant phenotype in GBM. Therefore, DRP1 could be a potential target for improving the effectiveness of radiation therapy.

Background

Glioblastoma multiforme (GBM, Word Health Organization grade IV glioma) is the most aggressive adult brain tumor and thus has the worst prognosis. Most of the patients (~ 70%) die within two years following diagnosis. Proper radiation therapy, meaning fractionated conformal three-dimensional radiotherapy to a total dose of 60 Gy in 30 daily fractions of 2 Gy, each was delivered. Such therapy, with the pre-radiation intake of an alkylating agent, temozolomide (TMZ), has improved treatment efficacy. However, the effects have been limited [1].

Advances in molecular biology have suggested that gain of oncogene function (e.g., N-ras, human epidermal growth factor receptor [EGFR]-1 [HER-1, also known as v-ErbB-2 avian erythroblastic leukaemia viral oncogene homolog 1, erbB-1] and isoforms 1 and 2 of citrate dehydrogenase [IDH1/2]) [2, 3], as well as the loss or inactivation of the function in tumor suppressor genes (e.g., p53, RB1, O^6-methylguanine-DNA-methyltransferase [MGMT], and phosphatase and tensin homolog [pTEN]) [4–7], are frequently associated with GBM. Although the oncogenic consequence is yet to be determined, risk factors in lifestyle (e.g., smoking, drinking habits and compulsive use of wireless phones) and environment (e.g., exposure to ionizing radiation and chemicals) have been implicated in the cumulative multigene alterations, which can then activate oncogene expression, induce aberrant cell growth and accelerate carcinogenic changes [8–12]. EGFR expression in GBM had attracted several provisional clinical trials targeted at EGFR-phosphatidylinositol 3-kinase (PI3K)-Akt/protein kinase B (PKB) and mammalian target of rapamycin (mTOR) signaling pathways as well as several related passages [13–15]. The preliminary results were promising; however, improvement of treatment efficacy and patient's survival were not as evident.

Hypoxia is an important factor for the increase of GBM resistance simply by inducing autophagy [16]. Biochemically, hypoxia not only activated nuclear translocation of apoptosis-related mitochondrial protein, BCL-2 nineteen kilo-Dalton interacting protein 3 (BNIP3) [17, 18], but also elevated synthesis of α-ketoglutarate and 2-hydroxyglutarate by IDH to increase chromatin epigenetic modification [19, 20], as well as resistance to treatment of TMZ and radiation [1, 7, 21]. Hypoxia also induced nuclear translocation of dynamin-related protein 1 (DRP1), which was associated with DNA repair-related protein, human homolog of yeast Rad23 protein A (hHR23A), by which the DRP1 could, on one hand, protect nucleoli and, on the other hand, increase DNA repair as well as cisplatin resistance of cancer cells [22, 23].

DRP1 is an 80-kDa GTPase, which mediates budding and scission of a variety of transport vesicles and organelles [22, 24, 25], including mitochondria [26]. A number of anticancer drugs, e.g., epipodophyllotoxins and cisplatin, induce mitochondrial fragmentation, a phenomenon that is closely associated with apoptosis and chemotherapeutic cytotoxicity [27]. A better understanding of DRP1 and the enzyme effect on drug activity could, therefore, provide more valuable information to improve disease management. In addition, these chemotherapeutic agents might become vital probes for studying the essential function as well as the regulation mechanism of DRP1 and other fusion/fission-related proteins in the intracellular material trafficking and organelle damage [22–25]. However, DRP1 has not been studied in the GBM.

In this study, we used immunohistochemistry and Western blotting to determine DRP1 expression in GBM. We then evaluated the prognostic significance of DRP1 expression in GBM patients. Moreover, we investigated the effect of shikonin and suberoylanilide hydroxamic acid (SAHA, vorinostat), a histone deacetylase (HDAC) inhibitor, on DRP1 expression as well as radiation sensitivity in vitro.

Results

1. **Overexpression of DRP1 in GBM specimens as determined by immunohistochemistry and Western blotting analysis**

From January 2008 to August 2012, 47 GBM patients who had undergone standard surgery and palliative radiation therapy with daily TMZ (75 mg/m^2) adjuvant monthly TMZ (150-200 mg/m^2) were retrospectively enrolled in the study. The demography and treatment parameters of these patients are listed in Table 1. Identification and classification of tissue staining are described in detail in the Materials and Methods section. Using immunohistochemical staining, the expression of DRP1 was detected in 41 (87.2%) of the Taiwanese GBM tumor specimens (Fig 1A, as crimson precipitates in the cytoplasm), and some of the DRP1 was identified in the nuclei of tumor cells (Fig 1B, DRP1-positive nuclei are shown as brown precipitates in the nuclei, compared to DRP1-negative blue nuclei) in 33 (80.5%) of the 41 samples. The positive and negative staining controls were shown in Supplementary S4A-S4C Figs. DRP1 signal

was detected in 32 (91.4%) of 35 American GBM patients, and nuclear DRP1 ($DRP1^{nuc+}$) was detected in 27 (84.4%) specimens. No difference was found in DRP1 expression between the American and Taiwanese GBM patients ($p = 0.609$). The expression of the 80-kDa DRP1 in Taiwanese patients was confirmed by Western blotting (Fig 1C). In addition, we speculated that the protein of DRP1-positive in nuclei is likely to the phosphorylated state of DRP1 (Supplementary S2C Figs). Interestingly, molecular weights of the DRP1 in 7 of 12 surgical specimens were higher than the anticipated 80-kDa and three samples clearly had two protein bands, indicating that the DRP1 in biopsies could be post-translationally modified [22]. It is worth mentioning that the anti-DRP1 monoclonal antibody has been proved and characterized, and is a highly specific antibody [22].

2. **The impact of DRP1 overexpression on GBM patient's prognosis**

The survival of patients with low DRP1 levels was significantly better than that of patients with high DRP1 levels. The difference between cumulative overall survival (OS) [$p = 0.0398$, 95% confidential interval (CI), 1.051-8.151; Hazard ratio (HR) between $DRP1^+$ and $DRP1^-$ patients was 5.71) were significant (Supplementary S1A & S1B Figs). The actual 18 month OS rate of $DRP1^+$ patients was 40.0%, while that of $DRP1^-$ patients was 80.0%. Survival of $DRP1^-$ patients was indeed better than $DRP1^+$ patients. When nuclear DRP1 was used as a perspective parameter, survival of patients with nuclear DRP1 was significantly worse than that of the other two groups (Fig 1D, $p = 0.0183$, log-rank test for trend; or Supplementary S1C and S1D Figs, OS, $p = 0.0039$, and PFS, $p < 0.0001$), indicating that expression of DRP1, including nuclear DRP1, could act as a prognostic phenotype of GBM. Subgroup analyses revealed that GBM patients with DRP1 overexpression and unmethylated MGMT promoter had the worst radiation responses and survival (Supplementary S1E & S1F Figs). At the time of data analysis (patients had been routinely followed for up to 24 months), 5 (83.3%) of 6 $DRP1^-$ patients were alive. Among these, four were progression-free.

3. **Silencing of DRP1 Expression in GBM Cells decreases cell growth, and mobility, but increases radiation sensitivity**

In vitro, protein levels of DRP1 were examined by Western blotting analysis in three human glioma cell lines (H4, U87MG and T98G). All three cell lines expressed both 80- and 85-kDa proteins (Fig 2A). Identities of the immunoprecipitated proteins were determined by matrix-assisted laser desorption/ionization-time-of-flight-mass spectrometry (MALDI-TOF). Peptide mass fingerprinting of both 80-kDa and 85-kDa proteins matched to DRP1: O00429, DRP1, indicating that both 80-kDa and 85-kDa proteins were DRP1 and that the 85-kDa protein could be post-translationally modified (Supplementary S2A-2D Figs). Furthermore, in the presence of calf intestinal phosphatase (CIP), the 85-kDa protein band

gradually disappeared, but the levels of the 80-kDa protein band increased, suggesting that the 85-kDa protein could be a phosphorylated form of 80-kDa DRP-1. (Supplementary S2 Fig)

As noted above, both pathological and clinical studies showed that higher DRP1 expression correlated with worse prognosis in patients concurrently treated with TMZ and irradiation. We, therefore, examined the effect of DRP1 on cell proliferation and migration. *In vitro*, inhibition of DRP1 expression by using shRNA to knockdown DRP1expression ($DRP1^{KD}$) (Fig 2B) reduced cell growth (Fig 2C) and mobility of tumor cells across matrigels (Fig 2D). Meanwhile, the decrease of cell mobility after lentivirus infection was not associated with cell viability. This was because the cell mobility assay used stable clones of lentivirus-infected cells, while the colony formation assay used cells following their infection with shLus or DRP-1KD lentivirus.

The current studies have provided that CD-133^{+} GBM stem cells retained more resistance than cancer cells to ionizing radiation [37, 38]. Silencing of DRP1, on the other hand, increased radiation sensitivity in both T98G (Fig 3A) and U87 cells (Fig 3B). The addition of TMZ only increased radiation sensitivity of $DRP1^{KD}$ T98G cells. The decrease in radiation resistance was about 5-10 folds. Interestingly, CD-133^{+} GBM stem cells (GSC) also highly expressed DRP1, in particular, the 85-kDa protein (Fig 3C). The silencing of DRP1 expression inhibited cell growth of GSC, including the number of cells and the spheroid formation (Fig 3D). These results confirmed our previous findings that DRP1, essential for mitochondrial protein import, was involved in cell growth and genotoxic resistance [22, 24, 25], suggesting that reducing total intracellular DRP1 expression or nuclear DRP1 levels could enhance anticancer efficacy of radiation and anticancer drug therapies.

4. The respective effects of shikonin and SAHA on DRP1 expression and cell survival

Our previous studies showed that DRP1 was involved in an alternative mitochondrial import, and disruption of this passage induces autophagy [24, 25]. Using DRP1 as a target, we found that several Chinese medicinal herbal extracts (CMHEs) inhibited DRP1 expression, including *Astragalus, propinquus*, *Koelreuteria elegans*, *Lithospermum erythrorhizon*, and *Polygala tenuifolia* [39]. Using the web engine (http://www.google.com.tw/) to search for the major ingredients of the plants, we found that shikonin from the *L. erythrorhizon* is one of the most promising pure compounds. To evaluate the effects of shikonin and DRP1 protein on the process of autophagy and apoptosis, we analyzed the related protein expression.

As shown in Fig 4A, shikonin decreased both 80- and 85-kDa DRP1, and increased autophagic marker, LC3B-II. Using fluorescence microscopy, shikonin clearly induced the formation of autophagosomes (Fig 4B). Although SAHA did not affect DRP1 expression (Fig 4C), it clearly increased levels of poly [ADP-ribose] polymerase 1 (PARP-1), a marker of apoptosis (Fig 4D, upper panel), but did not induce cleavage of PARP-1.

In DRP1^{KD} T98G cells, SAHA increased PARP-1 cleavage (Fig 4D, right-hand side) as well as cell death (Fig 4e right-panel) and mitochondria depolarization [Fig 4e left the panel, as shown by changes of mitochondrial membrane potential (MMP)]. After SAHA treatment, T98G cells were harvested and respectively analyzed by Western blotting and flow cytometry. Expression of b-actin was used as a monitoring standard for relative protein expression in the Western blotting analysis. Results are the means ± S.D. of three independent experiments. **, p <0.001

HDAC inhibitor does not influence the expression of DRP-1, including that of the total protein or the phosphorylated protein. However, under knockdown, the lower expression of DRP1 resulting from the artificial modification enlarged the cytotoxic effect of HDAC inhibitor, apparently through the induction of apoptosis and mitochondria depolarization, while at the same time moderating the suppression of autophagy. These data suggested that the DRP1 protein is likely to play a key role in HDAC inhibitor-mediated autophagy.

5. **Shikonin increases nuclear levels of anticancer drugs and arrests of DNA repair-related proteins in the perinuclear MAM**

Our previous studies showed that inhibiting intracellular cargo transportation-related enzymes could result in a reduction of nuclear levels of DNA repair-related proteins, such as ataxia-telangiectasia-mutated (ATM) kinase, and an increase of the cytotoxic effect of anticancer drugs and irradiation [22, 24, 25, 40]. Interestingly, using an Operatta® high content imaging system (PerkinElmer, Waltham, MA) to examine the effect of shikonin on the nuclear levels of 4',6-diamidino-2-phenylindole (DAPI) and daunorubicin, in T98G cells, we found that shikonin not only markedly increased nuclear DAPI and daunorubicin, but also significantly increased cell sensitivity to daunorubicin (Figs 5A-5C). We found that glioblastoma cells are not sensitive for daunorubicin in spite of it is not used for brain tumors. Moreover, shikonin treatment reduced the nuclear accumulation of ATM (Fig 5D, the left panel), supporting our former results that inhibition of DRP1 expression restricted the nuclear import of DNA repair-related enzymes and induced bulging of MAM (Fig 5D, right panel). Using a transmission electron microscopy, we further showed that shikonin treatment increased nuclear envelop damages (Figs 5E1 & 5E2).

Discussion

Our results show that DRP1 is highly expressed in newly diagnosed GBM patients (87.2%, 41/47). Moreover, nuclear DRP1 was identified in 33 (80.5%) of DRP1-positive (DRP1^{+}) pathological specimens. Using Western blotting to analyze DRP1 expression, we found that the molecular weights of DRP1 in 10 of 12 surgical samples were around 85-kDa. In spite of the number of analyzed patients are less, but it still moderated indicated that DRP1 in GBM biopsies could be post-translationally modified [16, 22]. Statistical analyses showed that patients with DRP1 overexpression or nuclear DRP1 (DRP1^{nuc+}) were more resistant to radiation and hence had a higher frequency of disease relapse and worse prognosis.

Subgroup statistics analyses revealed that GBM patients with DRP1 overexpression and unmethylated MGMT promoter had the worst radiation responses and survival (Supplementary S1E & S1F Figs).

In vitro, DRP1 expression correlates with resistant phenotype to radiation and TMZ (T98G cells were more resistant than U87MG cells). Nonetheless, silencing of DRP1 gene increases the sensitivity of both U87MG cells (with a methylated MGMT promoter) and T98G cells (with an unmethylated MGMT promoter) to radiation and TMZ, suggesting that the expression of DRP-1 increases the resistance to radiation, as well as that of Aldo-keto reductase (AKR) 1C1 and 1C2 [40, 41] to enforce radiation phenotype of GBM cells [22, 24, 25, 28, 29]. Binding of DRP1 to the nucleoli could further protect the rRNA-encoding region to maintain genome stability [22], and these events together could regulate cellular activity against cytotoxic agents and radiation. On the other hand, nuclear phosphorylated DRP-1 is likely to exhibit increased protein expression under hypoxia (Supplementary S2C Fig), as well as increased drug resistance [22].

Interestingly, the study reported that long-term exposure of GBM cells to TMZ decreases drug sensitivity by up-regulating the expression of AKR enzymes and glucose transporter [42]. Elevation of glucose transport altered mitochondrial metabolism, while the increase of AKR enzymes deactivated TMZ and cisplatin, supporting our findings that some of AKR enzymes were localized on the mitochondria-associated membrane (MAM), the essential organelle that regulated material transports to mitochondria and nucleus [39, 40]. Both transportation passages require DRP1, ATAD3A, and mitofusin 2 (Mfn2) [24, 25]. Since shikonin inhibits DRP1 expression in T98G cells, it is reasonable to believe that intracellular materials, such as proteins and lipids which are synthesized in the endoplasmic reticulum (ER), and scheduled to be transported to mitochondria and nucleus [22, 25], will be accumulated in the MAM. The lack of timely material supply would be difficult to maintain mitochondrial integrity, which could severely diminish the mitochondrial function and change the organelle morphology (Supplementary S3A-S3D Figs).

It is worth noting that mitochondria do not synthesize phosphatidylserine (PS) per se. The PS is mainly synthesized in the ER and MAM, and imported to the mitochondria. Vice versa, the phosphatidylethanolamine (PE), the unique phospholipid that is conjugated to autophagy-related gene 3 (Atg3) during initiation of autophagy, is converted from the PS in the mitochondria and transported back to the ER. Interestingly, the ER also constitutes the outer part of the nuclear envelope as well. It is, therefore, reasonable to anticipate that a decrease of cytoplasmic DRP1 may concurrently damage the mitochondrial membrane and the nuclear envelope, which not only decreases general ATP supply but also reduces nuclear imports of DNA repair-related enzymes [40]. Moreover, elevated nuclear import of DRP1 could consume massive intracellular hHR23A, which would competitively diminish the nuclear import of xeroderma pigmentosum complementation group C (XPC) to delay nucleotide excision repair (NER) that was essential for maintaining genome integrity following the challenge of TMZ or cisplatin [22, 40, 42, 43].

Both TMZ and radiation induce nuclear and mitochondrial genome DNA breakage. TMZ affects mitochondrial electron transports and oxidative phosphorylation as well [44]. Radiation, on the other hand, induces the translocation of ATM, which is important for the repair of DNA breaks, to the nucleus and mitochondria [45]. ATM deficiency, either by a genetic or a biochemical method, reduces genomic DNA repair function as well as mitochondrial biogenesis and oxidative respiratory function [46]. By demonstrating that extranuclear ATM bound to ER-associated peroxisome targeting signal type 1 (PTS1) receptor (also named peroxisomal biogenesis factor 5, Pex5), Watters et al suggested that besides nucleus, ATM could be targeting to the MAM [47]. In a gene knockout study, Baumgart et al further showed that defect in the Pex5 gene reduced peroxisomal metabolism, as well as expression and activities of mitochondrial respiration system [48]. Their results strongly suggested that MAM and its associated enzymes, in particular, the DRP1, a GTPase, played a pivotal role in allocating materials, which were essential for maintaining organelle morphology, and DNA integrity of the genome and the mitochondria. Our data supported their results and showed that reducing cytoplasmic DRP-1, either by addition of shikonin or exposure to hypoxia (Supplementary S4A-S4D Figs), might inhibit import of DNA repair-associated enzymes [40, 43] such as ATM and gamma-H2AX, and that of mitochondrial biogenesis- and oxidative respiration-related proteins to decrease genomic and mitochondrial DNA stability, which was ultimately reflected in an increased sensitivity to drugs and radiation.

Autophagy generally regarded as a rescue response under cells including both normal cells and tumor cells, are confronted with danger, such as starvation, irradiation exposure. The inhibition of DRP1 significant increased the radiation sensitivity and repressed the autophagy response under cells faced chemo-treatment (Figs. 3AB, 4C), at the same time, DRP1-KD led to an increase apoptosis response of glioblastoma cells (Fig. 4D). Obviously, the lack of DRP1 similar to the inhibition of autophagy contributed to the cell's sensitivity to both chemo- and radio-resistance [49]. In spite of this study couldn't explain clearly the played role of DRP1 in the autophagy process, while revealing evidence of light is likely to the DRP1 participated with mitochondrial DNA stability (Fig. 4e) [49].

Conclusions

In conclusion, our results showed that DRP1 was overexpressed in GBM. The inhibition of DRP1 expression induces autophagy and enhances radiation sensitivity. This effect is specific to cancer cells, which overexpress not only DRP1 but also ATAD3A, AKR1C1, eukaryotic elongation factor (eEF2) and optic atrophy 1 (OPA1), a condition that is not detected in non-tumor counterpart [28, 50, 51]. In fact, this is the first report on the DRP-1 expression and clinical characteristics of a large series of glioma patients of high-grade. In addition to inducing autophagy, silencing of DRP1 reduced cell growth and invasion potentials, and such features were also found in GBM stem cells. Reducing DRP1 expression augmented the cytotoxicity to SAHA (acetylation and apoptosis-inducing agent) and daunorubicin as well. Although the size of this study population was small, our data shed some light on the radio-resistant phenotype of GBM, of which DRP1 could be a potential marker; though DRP1 alone might not be an independent prognostic factor.

Abbreviations

Abbreviations used are
ATAD3A, the ATPase family, AAA domain containing 3A; CIM, confocal immunofluorescence microscopy; DRP1, dynamin-related protein 1; ER, endoplasmic reticulum; GBM, glioblastoma multiforme; hHR23A, human homolog of yeast Rad23 protein A; IDH1, isocitrate dehydrogenase 1; MAM, mitochondria-associated membrane; MGMT, O^6-methylguanine-DNA-methyltransferase; SAHA, suberoylanilide hydroxamic acid (vorinostat); TMZ, temozolomide

Declarations

Ethics approval and consent to participate: The protocol of the study, including tissue specimen collection, pathology evaluation, the methylation status of O(6)-methylguanine-DNA methyltransferase (MGMT) promoter and survival assessment, was approved by the Medical Ethics Committee of Taichung Veterans General Hospital (Approval number: CF12026B#2).

Consent for publication: Not applicable.

Availability of data and materials: All relevant data have been uploaded to DRYAD and can be accessed using the following link: https://datadryad.org/review?d oi = doi 10.5061 / dryad.d025q4p

Competing Interests: The funders had no role in study design, data collection, and analysis, decision to publish, or preparation of the manuscript. None of the authors received a salary from the above funders. All of the authors declare no conflicts of interest.

Financial Disclosure

The funders had no role in study design, data collection and analysis, decision to publish, or preparation of the manuscript.

Authors' Contributions

Conception and Design: WY Cheng, KC Chow, CC Shen; **Development of methodology:** KC Chow; **Acquisition of data:** WY Cheng, CC Shen; **Analysis and interpretation of data:** WY Cheng, MT Chiao, YC

Yang, KC Chow; **Writing and review:** WY Cheng, KC Chow, CC Shen; **Administrative, technical or material support:** WY Cheng, KC Chow. All authors read and approved the manuscript.

Author details: [1] Institute of Biomedical Sciences, National Chung Hsing University, Taichung, Taiwan; [2]Division of Minimally Invasive Neurosurgery, Neurological Institute, Taichung Veterans General Hospital, Taichung 40705, Taiwan; [3]Department of Physical Therapy, Hung Kuang University, Taichung 43302, Taiwan; [4]Graduate Institute of Biomedical Sciences, and [5]Agricultural Biotechnology Centre, National Chung Hsing University, Taichung, Taiwan; [6]Department of Medicine, and Graduate Institute of Medical Sciences, National Defence Medical Centre, Taipei, Taiwan; [7]Tri-Service General Hospital, National Defence Medical Centre, Taipei, Taiwan. [8] Department of Game and Product Design, Chienkuo Technology University, Taiwan[9]Basic Medical Education Center, Central Taiwan University of Science and Technology, Taichung, Taiwan. WY Cheng [1,2,3,] e-mail: wycheng07@yahoo.com.tw, KC Chow [4,5,] e-mail: kcchow@dragon.nchu.edu.tw, MT Chiao[2] e-mail: mtchiao@gmail.com , YC Yang[2] e-mail: jean1007@gmail.com; CC Shen[*,2,3,6,7,8,9] e-mail: ccshen61093@gmail.com

References

1.
Stupp R, Hegi ME, Mason WP, van den Bent MJ, Taphoorn MJ, Janzer RC, Ludwin SK, Allgeier A, Fisher B, Belanger K, et al. Effects of radiotherapy with concomitant and adjuvant temozolomide versus radiotherapy alone on survival in glioblastoma in a randomised phase III study: 5-year analysis of the EORTC-NCIC trial. Lancet Oncol. 2009;10(5):459–66.
2.
Shinojima N, Tada K, Shiraishi S, Kamiryo T, Kochi M, Nakamura H, Makino K, Saya H, Hirano H, Kuratsu J, et al. Prognostic value of epidermal growth factor receptor in patients with glioblastoma multiforme. Cancer Res. 2003;63(20):6962–70.
3.
Sanson M, Marie Y, Paris S, Idbaih A, Laffaire J, Ducray F, El Hallani S, Boisselier B, Mokhtari K, Hoang-Xuan K, et al. Isocitrate dehydrogenase 1 codon 132 mutation is an important prognostic biomarker in gliomas. J Clin Oncol. 2009;27(25):4150–4.
4.
Ichimura K, Schmidt EE, Goike HM, Collins VP. Human glioblastomas with no alterations of the CDKN2A (p16INK4A, MTS1) and CDK4 genes have frequent mutations of the retinoblastoma gene. Oncogene. 1996;13(5):1065–72.
5.
Wang SI, Puc J, Li J, Bruce JN, Cairns P, Sidransky D, Parsons R. Somatic mutations of PTEN in glioblastoma multiforme. Cancer Res. 1997;57(19):4183–6.
6.

Fulci G, Labuhn M, Maier D, Lachat Y, Hausmann O, Hegi ME, Janzer RC, Merlo A, Van Meir EG. p53 gene mutation and ink4a-arf deletion appear to be two mutually exclusive events in human glioblastoma. Oncogene. 2000;19(33):3816–22.
7.
Spiegl-Kreinecker S, Pirker C, Filipits M, Lotsch D, Buchroithner J, Pichler J, Silye R, Weis S, Micksche M, Fischer J, et al. O6-Methylguanine DNA methyltransferase protein expression in tumor cells predicts outcome of temozolomide therapy in glioblastoma patients. Neuro Oncol. 2010;12(1):28–36.
8.
Efird JT, Friedman GD, Sidney S, Klatsky A, Habel LA, Udaltsova NV, Van den Eeden S, Nelson LM. The risk for malignant primary adult-onset glioma in a large, multiethnic, managed-care cohort: cigarette smoking and other lifestyle behaviors. J Neurooncol. 2004;68(1):57–69.
9.
Hardell L, Carlberg M, Hansson Mild K. Epidemiological evidence for an association between use of wireless phones and tumor diseases. Pathophysiology. 2009;16(2–3):113–22.
10.
Efird JT. Season of birth and risk for adult onset glioma. Int J Environ Res Public Health. 2010;7(5):1913–36.
11.
Baglietto L, Giles GG, English DR, Karahalios A, Hopper JL, Severi G. Alcohol consumption and risk of glioblastoma; evidence from the Melbourne Collaborative Cohort Study. Int J Cancer. 2011;128(8):1929–34.
12.
Carlberg M, Hardell L. On the association between glioma, wireless phones, heredity and ionising radiation. Pathophysiology. 2012;19(4):243–52.
13.
Haas-Kogan DA, Prados MD, Tihan T, Eberhard DA, Jelluma N, Arvold ND, Baumber R, Lamborn KR, Kapadia A, Malec M, et al. Epidermal growth factor receptor, protein kinase B/Akt, and glioma response to erlotinib. J Natl Cancer Inst. 2005;97(12):880–7.
14.
Huang TT, Sarkaria SM, Cloughesy TF, Mischel PS. Targeted therapy for malignant glioma patients: lessons learned and the road ahead. Neurotherapeutics. 2009;6(3):500–12.
15.
Ohka F, Natsume A, Wakabayashi T. Current trends in targeted therapies for glioblastoma multiforme. Neurol Res Int. 2012;2012:878425.
16.
Hu YL, DeLay M, Jahangiri A, Molinaro AM, Rose SD, Carbonell WS, Aghi MK. Hypoxia-induced autophagy promotes tumor cell survival and adaptation to antiangiogenic treatment in glioblastoma. Cancer Res. 2012;72(7):1773–83.
17.

Burton TR, Henson ES, Baijal P, Eisenstat DD, Gibson SB. The pro-cell death Bcl-2 family member, BNIP3, is localized to the nucleus of human glial cells: Implications for glioblastoma multiforme tumor cell survival under hypoxia. Int J Cancer. 2006;118(7):1660–9.
18.
Daido S, Kanzawa T, Yamamoto A, Takeuchi H, Kondo Y, Kondo S. Pivotal role of the cell death factor BNIP3 in ceramide-induced autophagic cell death in malignant glioma cells. Cancer Res. 2004;64(12):4286–93.
19.
Wise DR, Ward PS, Shay JE, Cross JR, Gruber JJ, Sachdeva UM, Platt JM, DeMatteo RG, Simon MC, Thompson CB. Hypoxia promotes isocitrate dehydrogenase-dependent carboxylation of alpha-ketoglutarate to citrate to support cell growth and viability. Proc Natl Acad Sci U S A. 2011;108(49):19611–6.
20.
Ward PS, Thompson CB. Metabolic reprogramming: a cancer hallmark even warburg did not anticipate. Cancer Cell. 2012;21(3):297–308.
21.
Wang H, Cai S, Ernstberger A, Bailey BJ, Wang MZ, Cai W, Goebel WS, Czader MB, Crean C, Suvannasankha A, et al. Temozolomide-mediated DNA methylation in human myeloid precursor cells: differential involvement of intrinsic and extrinsic apoptotic pathways. Clin Cancer Res. 2013;19(10):2699–709.
22.
Chiang YY, Chen SL, Hsiao YT, Huang CH, Lin TY, Chiang IP, Hsu WH, Chow KC. Nuclear expression of dynamin-related protein 1 in lung adenocarcinomas. Mod Pathol. 2009;22(9):1139–50.
23.
Sudhakar JN, Chow KC. Human RAD23 homolog A is required for the nuclear translocation of apoptosis-inducing factor during induction of cell death. Biol Cell. 2014;106(10):359–76.
24.
Fang HY, Chang CL, Hsu SH, Huang CY, Chiang SF, Chiou SH, Huang CH, Hsiao YT, Lin TY, Chiang IP, et al. ATPase family AAA domain-containing 3A is a novel anti-apoptotic factor in lung adenocarcinoma cells. J Cell Sci. 2010;123(Pt 7):1171–80.
25.
Chiang SF, Huang CY, Lin TY, Chiou SH, Chow KC. An alternative import pathway of AIF to the mitochondria. Int J Mol Med. 2012;29(3):365–72.
26.
Taguchi N, Ishihara N, Jofuku A, Oka T, Mihara K. Mitotic phosphorylation of dynamin-related GTPase Drp1 participates in mitochondrial fission. J Biol Chem. 2007;282(15):11521–9.
27.
Tacka KA, Szalda D, Souid AK, Goodisman J, Dabrowiak JC. Experimental and theoretical studies on the pharmacodynamics of cisplatin in jurkat cells. Chem Res Toxicol. 2004;17(11):1434–44.
28.

Chen TC, Hung YC, Lin TY, Chang HW, Chiang IP, Chen YY, Chow KC. Human papillomavirus infection and expression of ATPase family AAA domain containing 3A, a novel anti-autophagy factor, in uterine cervical cancer. Int J Mol Med. 2011;28(5):689–96.
29.
Huang KH, Chow KC, Chang HW, Lin TY, Lee MC. ATPase family AAA domain containing 3A is an anti-apoptotic factor and a secretion regulator of PSA in prostate cancer. Int J Mol Med. 2011;28(1):9–15.
30.
Remmele W, Schicketanz KH. Immunohistochemical determination of estrogen and progesterone receptor content in human breast cancer. Computer-assisted image analysis (QIC score) vs. subjective grading (IRS). Pathol Res Pract. 1993;189(8):862–6.
31.
Smith JS, Alderete B, Minn Y, Borell TJ, Perry A, Mohapatra G, Hosek SM, Kimmel D, O'Fallon J, Yates A, et al. Localization of common deletion regions on 1p and 19q in human gliomas and their association with histological subtype. Oncogene. 1999;18(28):4144–52.
32.
Chiao MT, Cheng WY, Yang YC, Shen CC, Ko JL. Suberoylanilide hydroxamic acid (SAHA) causes tumor growth slowdown and triggers autophagy in glioblastoma stem cells. Autophagy. 2013;9(10):1509–26.
33.
Cheng WY, Chiao MT, Liang YJ, Yang YC, Shen CC, Yang CY. Luteolin inhibits migration of human glioblastoma U-87 MG and T98G cells through downregulation of Cdc42 expression and PI3K/AKT activity. Mol Biol Rep. 2013;40(9):5315–26.
34.
Ishiyama M, Tominaga H, Shiga M, Sasamoto K, Ohkura Y, Ueno K. A combined assay of cell viability and in vitro cytotoxicity with a highly water-soluble tetrazolium salt, neutral red and crystal violet. Biol Pharm Bull. 1996;19(11):1518–20.
35.
EL K. P M: Nonparamertric estimation form incomplete observations. j Am Stat Assoc. 1958;53(282):457–81.
36.
N M: Evaluation of survival data and two new rank order statistics arising in its consideration. Cancer Chemother Rep 1966, 50(3):163–170.
37.
Steponkiene S, Kavaliauskiene S, Purviniene R, Rotomskis R, Juzenas P. Quantum dots affect expression of CD133 surface antigen in melanoma cells. Int J Nanomedicine. 2011;6:2437–44.
38.
Ma HI, Chiou SH, Hueng DY, Tai LK, Huang PI, Kao CL, Chen YW, Sytwu HK. Celecoxib and radioresistant glioblastoma-derived CD133 + cells: improvement in radiotherapeutic effects. Laboratory investigation. J Neurosurg. 2011;114(3):651–62.
39.

Chiang YY, Wang SL, Yang CL, Yang HY, Yang HC, Sudhakar JN, Lee CK, Huang HW, Chen CM, Chiou SH, et al. Extracts of Koelreuteria henryi Dummer induce apoptosis and autophagy by inhibiting dihydrodiol dehydrogenase, thus enhancing anticancer effects. Int J Mol Med. 2013;32(3):577–84.
40.
You WC, Chiou SH, Huang CY, Chiang SF, Yang CL, Sudhakar JN, Lin TY, Chiang IP, Shen CC, Cheng WY, et al. Mitochondrial protein ATPase family, AAA domain containing 3A correlates with radioresistance in glioblastoma. Neuro Oncol. 2013;15(10):1342–52.
41.
Deng HB, Parekh HK, Chow KC, Simpkins H. Increased expression of dihydrodiol dehydrogenase induces resistance to cisplatin in human ovarian carcinoma cells. J Biol Chem. 2002;277(17):15035–43.
42.
Le Calve B, Rynkowski M, Le Mercier M, Bruyere C, Lonez C, Gras T, Haibe-Kains B, Bontempi G, Decaestecker C, Ruysschaert JM, et al. Long-term in vitro treatment of human glioblastoma cells with temozolomide increases resistance in vivo through up-regulation of GLUT transporter and aldo-keto reductase enzyme AKR1C expression. Neoplasia. 2010;12(9):727–39.
43.
Lai TC, Chow KC, Fang HY, Cho HC, Chen CY, Lin TY, Chiang IP, Ho SP. Expression of xeroderma pigmentosum complementation group C protein predicts cisplatin resistance in lung adenocarcinoma patients. Oncol Rep. 2011;25(5):1243–51.
44.
Oliva CR, Nozell SE, Diers A, McClugage SG 3rd, Sarkaria JN, Markert JM, Darley-Usmar VM, Bailey SM, Gillespie GY, Landar A, et al. Acquisition of temozolomide chemoresistance in gliomas leads to remodeling of mitochondrial electron transport chain. J Biol Chem. 2010;285(51):39759–67.
45.
Ambrose M, Goldstine JV, Gatti RA. Intrinsic mitochondrial dysfunction in ATM-deficient lymphoblastoid cells. Hum Mol Genet. 2007;16(18):2154–64.
46.
Kim WJ, Vo QN, Shrivastav M, Lataxes TA, Brown KD. Aberrant methylation of the ATM promoter correlates with increased radiosensitivity in a human colorectal tumor cell line. Oncogene. 2002;21(24):3864–71.
47.
Watters D, Kedar P, Spring K, Bjorkman J, Chen P, Gatei M, Birrell G, Garrone B, Srinivasa P, Crane DI, et al. Localization of a portion of extranuclear ATM to peroxisomes. J Biol Chem. 1999;274(48):34277–82.
48.
Baumgart E, Vanhorebeek I, Grabenbauer M, Borgers M, Declercq PE, Fahimi HD, Baes M. Mitochondrial alterations caused by defective peroxisomal biogenesis in a mouse model for Zellweger syndrome (PEX5 knockout mouse). Am J Pathol. 2001;159(4):1477–94.
49.
Bo T, Yamamori T, Suzuki M, Sakai Y, Yamamoto K, Inanami O. Calmodulin-dependent protein kinase II (CaMKII) mediates radiation-induced mitochondrial fission by regulating the phosphorylation of dynamin-

related protein 1 (Drp1) at serine 616. Biochem Biophys Res Commun. 2018;495(2):1601–7.
50.
Hsu NY, Ho HC, Chow KC, Lin TY, Shih CS, Wang LS, Tsai CM. Overexpression of dihydrodiol dehydrogenase as a prognostic marker of non-small cell lung cancer. Cancer Res. 2001;61(6):2727–31.
51.
Fang HY, Chen CY, Chiou SH, Wang YT, Lin TY, Chang HW, Chiang IP, Lan KJ, Chow KC. Overexpression of optic atrophy 1 protein increases cisplatin resistance via inactivation of caspase-dependent apoptosis in lung adenocarcinoma cells. Hum Pathol. 2012;43(1):105–14.

Methods

1. Tissue specimens and immunohistochemical detection of DRP1 expression.

From January 2008 to August 2012, tissue specimens were collected from 47 patients with newly diagnosed glioblastoma multiforme (GBM). The protocol of the study, including tissue specimen collection, pathology evaluation, the methylation status of O(6)-methylguanine-DNA methyltransferase (MGMT) promoter and survival assessment, was approved by the Medical Ethics Committee of Taichung Veterans General Hospital (Approval number: CF12026B#2). Tissue microarrays of 35 American GBM samples (GL806, US Biomax, Inc., Rockville, MD, USA) were used to compare DRP1 expression between Taiwanese and American patients. Immunohistological staining was performed on formalin-fixed sections using an LSAB method (DAKO, Carpenteria, CA). The chromogenic reaction was visualized by peroxidase-conjugated streptavidin and aminoethyl carbazole (Sigma, St. Louis, MO) [22, 24, 25, 28, 29]. Slides were evaluated by at least two independent pathologists without knowledge of the patient's clinicopathological background. An immune-reaction scoring system was used for scoring [30]. DRP1 expression was assessed in non-necrotic tumor areas of five separate microscopic fields of view under a magnification of 40X and was classified as the mean of the percentage of DRP1 immunohistochemical positive tumor cells. DRP1 expression was ranked as: <25, 25-50, 51-75 and >75% DRP1-positive tumor cells. The associated kappa statistics revealed a good interobserver agreement of k = 0.81. A specimen was considered having strong signals when more than 50% of cancer cells were positively stained; intermediate signals, if 25-50% cells stained positive; weak, if the positive cells were between 10 and 25%; and negative, if less than 10% cells were stained. Cases with strong and intermediate signals (≥ 25% cells positive) were classified as $DRP1^{+}$, those with weak or negative DRP1 signals were classified as $DRP1^{-}$.

2. Cell culture and alteration of DRP1 expression using lentivirus-carrying shRNA or ectopic plasmid.

Human glioblastoma multiforme cell line, H4, U87MG ,and T98G were obtained from ATCC (Manassas, VA, USA) and grown in Dulbecco modified Eagle medium (DMEM) supplemented with 10% fetal bovine serum (FBS), 4 mM glutamine, 100 U/ml penicillin and 100 μg/ml streptomycin. The cells were routinely tested and authenticated using a PromegaGenePrint® 10 system for human cell line DNA typing (Mission Biotech, Taipei, Taiwan). Among these three cell lines, we have proven in line with the correct both human

glioblastoma lineages of U87MG and T98G cell using short tandem repeat (STR) assay performed by Third-party research institution, whiles H4 cells don't been executed (Supplementary S6 & S7 Figs). The cells were grown to 80% confluence on the day of infection. Lentivirus carrying DRP1 shRNA was prepared using a three-plasmid transfection method [31]. The product lentivirus was used to infect U87MG and T98G cells, and cells with DRP1 gene knockdown ($DRP1^{KD}$) were selected using 1 μg/ml puromycin. After lentivirus infection including infection with sh-Luc and $DRP\text{-}1^{KD}$, the attached cells were detached by treatment with trypsin and reseeded at 100, 500, 2,000, and 5,000 cells/well of culture plate, respectively. The cells were incubated at 37°C for 10 days, visible colonies that contained more than 50 cells were counted and the plating efficiency was determined. A semi-log graph of the cell survival fractions (ratio of colonies formed by lentivirus infected cells to colonies formed by control cells) against radiation dosage was plotted. (Fig 2C).

3. Western blotting analysis.

Western blotting analysis has been described previously [22, 24, 25, 28, 29]. Briefly, 30 μg of total cell lysate was separated on a 10% polyacrylamide gel with a 4.5% stacking gel. After electrophoresis, proteins were transferred to a nitrocellulose membrane. The membrane was probed with specific antibodies. The protein was visualized by exposing the membrane to an X-Omat film with enhanced chemiluminescence reagent (Merck, Darmstadt, Germany). The respective primary antibodies were mouse anti-DRP1, and mouse anti-b-actin. Mouse monoclonal antibodies to DRP1 were home-made and had been characterized [22]. The digital images on X-Omat film were processed in Adobe Photoshop 7.0 (http://www.adobe.com/). The results were analyzed and quantified by the software, image-J (NIH, Bethesda, MD).

4. Confocal immunofluorescence microscopy.

Purified shikonin (>98%, HPLC) was purchased from Sigma-Aldrich (Saint Louis, Mo). The method for immunofluorescence confocal microscopy had been described previously [22, 24, 25]. Briefly, the cells on slides were fixed with 4% paraformaldehyde for 15 min at room temperature and permeabilized with 0.1% Triton X-100 prior to staining with mouse anti-DRP1. After washing off of the primary antibodies, slides were incubated with Alexa 488-conjugated goat anti-rabbit IgG (Invitrogen, Grand Island, NY). The nuclei were stained with 4', 6-Diamidino-2-phenylindole (DAPI) and the slides were examined under a laser confocal microscope (Olympus FV-1000, Tokyo, Japan). Images of the cells were analyzed by FV10-ASW 3.0 software (Tokyo, Japan).

5. Colony formation assay and the culture of GBM stem cells.

T98G, T98G-$DRP1^{KD}$, GBM stem cells (GSC), and GSC-$DRP1^{KD}$ cells were separately treated with 3, 6, or 12 Greys (Gy) of radiation (Varian 21EX linear accelerator, Varian Oncology Systems, Palo Alto, CA). For colony formation assays, after radiation or infection with a lentivirus, the attached cells were detached by treatment with trypsin and reseeded at 100, 500, 2,000, and 5,000 cells/well of culture plate, respectively. The cells were incubated at 37°C for 10 days, visible colonies that contained more than 50 cells were

counted and the plating efficiency was determined. Semi-log graph of the cell survival fractions (ratio of colonies formed by irradiated cells to colonies formed by control cells) against radiation dosage was plotted. The glioblastoma stem cell (GSC) was prepared according to the previously described protocol [32]. In brief, the obtained tissues were washed and enzymatically dissociated into individual cells. The dissociated cells were cultured in neurosphere-conditioned medium using Neurobasal media (Invitrogen, 21103-049) containing N2 and B27 supplements (Invitrogen, 17502-048; 0080085SA), plus human recombinant bFGF and EGF (50 ng/ml each; R&D Systems, 233-FB; 236-EG). After 2 to 4 weeks incubation, serial dilution was performed on the surviving GSCs to select a single cell that was able to grow a new sphere. The glioblastoma stem cells (GSCs), spheroid type, were cultured in neurosphere-conditioned medium (NSC medium).

6. The cell mobility of cells across matrigel assay.

The mobility of infected lentiviruses including both shLuc and DRP-1KD in U-87 MG and T98G cells was measured with the modified Boyden chamber containing Matrigel gel (BD Biosciences, USA) [33], with the well of chambers including a membrane with 8 μm pores. The Matrigel assay was performed according to the protocol suggested by BD Biosciences. Briefly, a vial of BD matrigelTM basement membrane matrix (BD-MBM, 356234) was thawed on ice overnight, and then diluted to ½ and ¼ with ice-cold serum-free Dulbecco's modified Eagle's medium (DMEM). Five ml of the diluted BD-MBM was spread in a petri dish on ice, before a piece of polycarbonate membrane (with 5.0 μm pore size) was submerged into the suspension mixture. Membrane coating was performed at room temperature for one hour. The membrane was rinsed with serum-free DMEM once and then mounted onto the Boyden chamber.

The lower chamber contained the 4% FBS medium. 1 $\times 10^5$ cells were pipeted into the well of the upper chamber at intervals of one hr for 8 hr and then incubated at 37°C for 24 hr in a humidified incubator with 5% CO_2. Following complete removal of the non-invading cells, the membrane was lifted from the chamber, and fixed in 100% methanol for 2 min. The cells on the membrane were stained with 1% toluidine blue for 2 min and washed twice with distilled water. After counting the cells, the percent invasion on the membrane was calculated by comparing the experimental group to the control group.

To count the cells in the lower chamber, the medium was carefully removed, and replaced with 100 μl of PBS with WST-1 (BioVision, Mountain View, CA) solution. The reaction was incubated at 37°C for 1-4 hr in a humidified incubator with 5% CO_2. Each experiment was done in triplicate, and the optical absorbance (450/620, in a SunriseTM, Tecan, microplate absorbance reader) was measured by coloration of the reacted substrate, which was catalyzed by mitochondrial dehydrogenases. The percent invasion and invasion index in the chamber were calculated by comparing the experimental group to the control group.

A polycarbonate membrane without Matrigel coating was used for cell trans-well study.

7. Drug-sensitivity assay.

Drug-sensitivity was measured by a WST-1 assay [34]. Cells were seeded at 100, 1,000, and 5,000 cells/96-well plates 18 hr prior to drug challenge. Cells were pulse-treated with 4 μM of daunorubicin for 2 hr. The negative control cells were treated with the solvent for the drug. Total survival of the cells was determined 72 hr following drug challenge, and percent survival was estimated by dividing optical absorbance resulted from each experiment group with that of the control group. Each experiment was done in triplicates, and the optical absorbance was measured by the coloration of the reacted substrate, WST-1 (BioVision, Mountain View, CA), which was catalyzed by mitochondrial dehydrogenases.

8. Statistical analysis.

Overall survival (OS) was the time from the date of diagnosis to the date of death. Survival curves were plotted using the Kaplan-Meier estimator [35] and the statistical difference in survival between the different groups was compared by a log-rank test [36]. Statistical tests were two-sided, and $p < 0.05$ was considered significant. The *t*-test was utilized to compare the numerical difference of clinical parameters. Differences in patients' performance status, tumor location, and surgical resection status were assessed by c-square or Fisher's exact test. Analyses of the data were performed using SPSS 10.3 software (Chicago, IL).

Tables

Table 1. The correlation among DRP-1 expression and various patient characteristics.

	Patients (n=47)		DRP-1nuc$^+$ (n=33)		DRP-1cyt$^+$ (n=8)		DRP-1$^-$ (n=6)		*p* value
	n	%	n	%	n	%	n	%	
Age									0.534
≦60	25	(53.2%)	18	(54.5%)	3	(37.5%)	4	(66.7%)	
>60	22	(46.8%)	15	(45.5%)	5	(62.5%)	2	(33.3%)	
Gender									0.221
Male	22	(46.8%)	16	(48.5%)	5	(62.5%)	1	(16.7%)	
Female	25	(53.2%)	17	(51.5%)	3	(37.5%)	5	(83.3%)	
Tumor number									0.101
Solitary	43	(91.5%)	32	(97.0%)	6	(75.0%)	5	(83.3%)	
Multiple	4	(8.5%)	1	(3.0%)	2	(25.0%)	1	(16.7%)	
Tumor size									0.305
≦3cm	5	(10.6%)	5	(15.2%)	0	(0.0%)	0	(0.0%)	
>3cm	42	(89.4%)	28	(84.8%)	8	(100.0%)	6	(100.0%)	
Tumor occurrence									0.177
Primary	41	(87.2%)	29	(87.9%)	8	(100.0%)	4	(66.7%)	
Recurrence	6	(12.8%)	4	(12.1%)	0	(0.0%)	2	(33.3%)	

Chi-square test. *p<0.05, **p<0.01

Figures

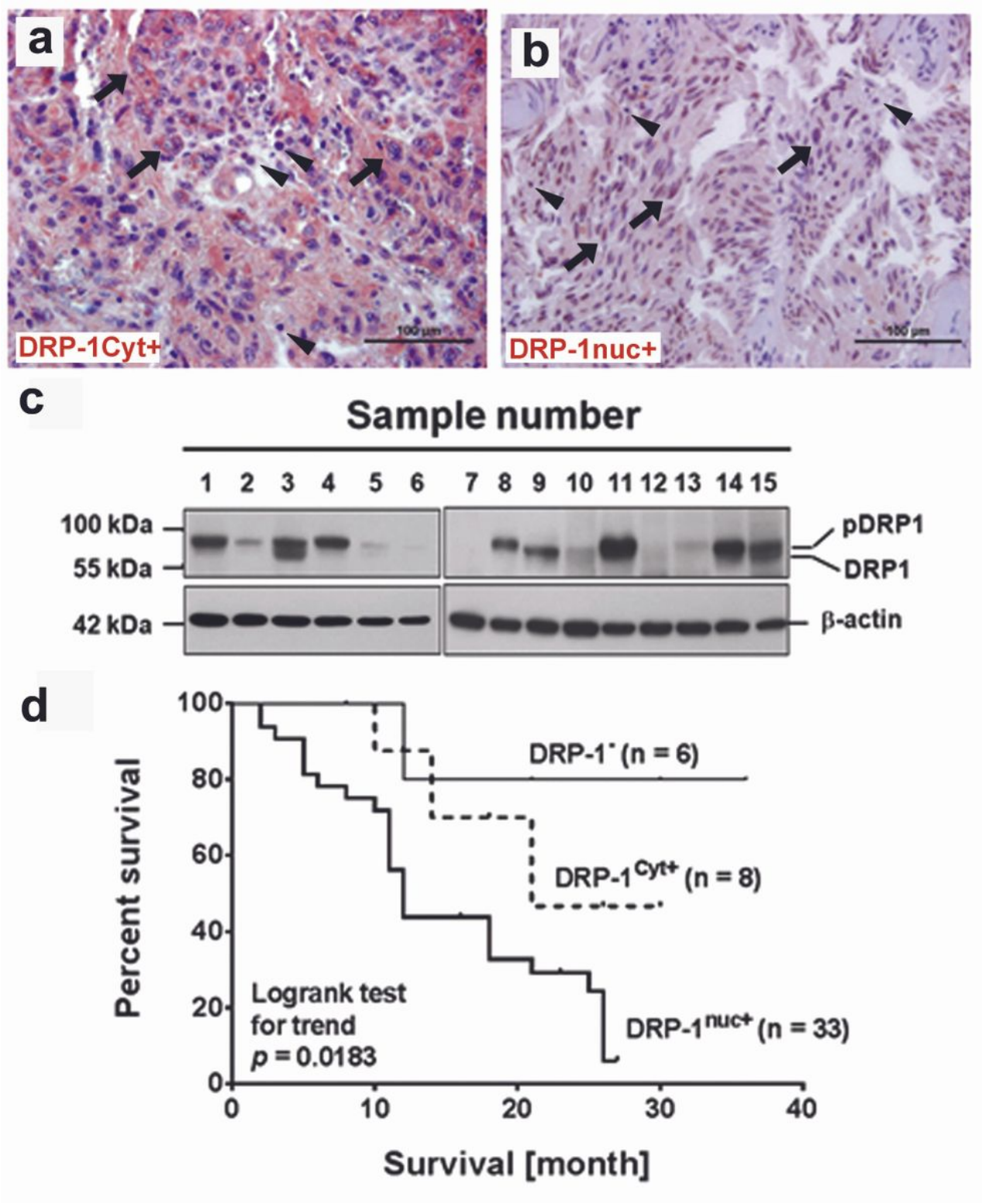

Figure 1

Immunohistochemical staining for the detection of DRP1 expression in GBM pathological specimens. In Taiwanese patients, (A) GBM tumor tissues highly expressed DRP1 (as crimson precipitates in the cytoplasm, denoted as DRP1cyt+) and (B) highly expressed nuclear DRP1 (as brown precipitates in the nuclei, denoted as DRP1nuc+) (original magnification □ 400). The slides were counterstained with hematoxylin. (The positive and negative controls were shown in the Supplementary S5A-S5C Figs.) The

black arrows indicate DRP1 staining in tumor cells. The white arrowheads indicate the infiltration of immune cells. Scale bars are 100 □m. (C) Expression levels of DRP1 in surgically resected GBM specimens as determined by Western blotting. The calculated molecular weight of DRP1 was 80-kDa, and the 85-kDa protein bands are probably the phosphorylated DRP1. (D) Comparison of Kaplan-Meier product limit estimates of survival analysis in patients with GBM. Patients were divided into three groups, DRP1nuc+, DRP1cyt+ and DRP1-, according to the expression and location of DRP1. The statistical difference in survival among the three groups was compared by a log-rank test for trend. DRP1nuc+ patients (higher nuclear DRP1 expression) had significantly shorter OS ($p = 0.0183$). (For other survival comparisons, please check the Supplementary S1A to S1E Figs).

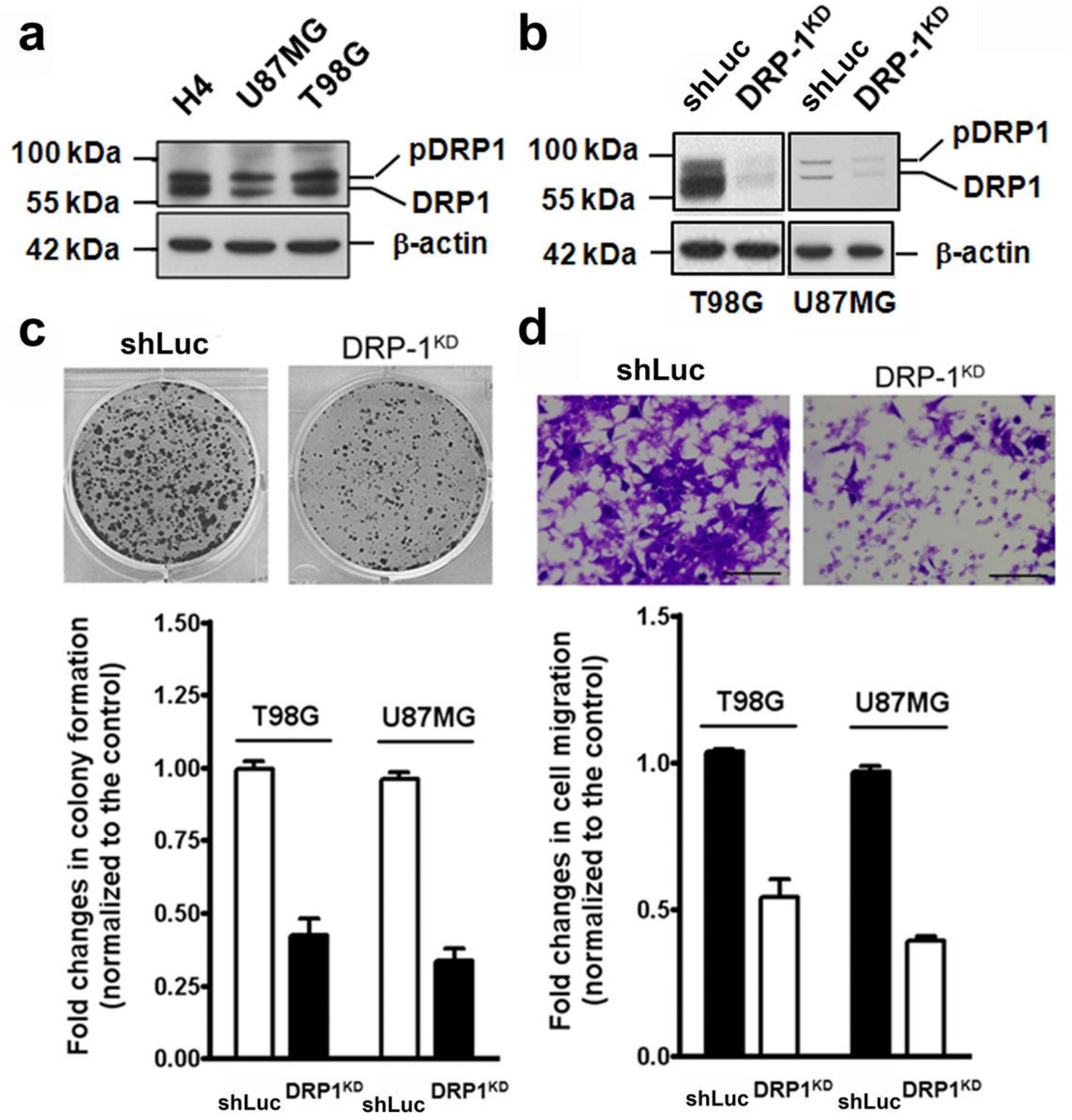

Figure 2

Correlation of DRP1 expression with cell growth and invasion potential of GBM cells. (A) DRP1 was highly expressed in human H4 and T98G glioblastoma cells. DRP1 level in U87MG was lower than that in T98G cells. (B) The silencing of DRP1 expression (DRP1KD) reduced the DRP1 protein level (as detected by Western blotting) of the T98G and U87MG cells. (C) The silencing of DRP1 expression decreased proliferation capacity (as measured by colony formation and WST-1 assays). (D) DRP1KD T98G and

DRP1KD U87MG cells had lower invasion potential (as measured by matrigel penetration assay) Scale bars are 250 m. The results were repeated over three independent experiments in each case.

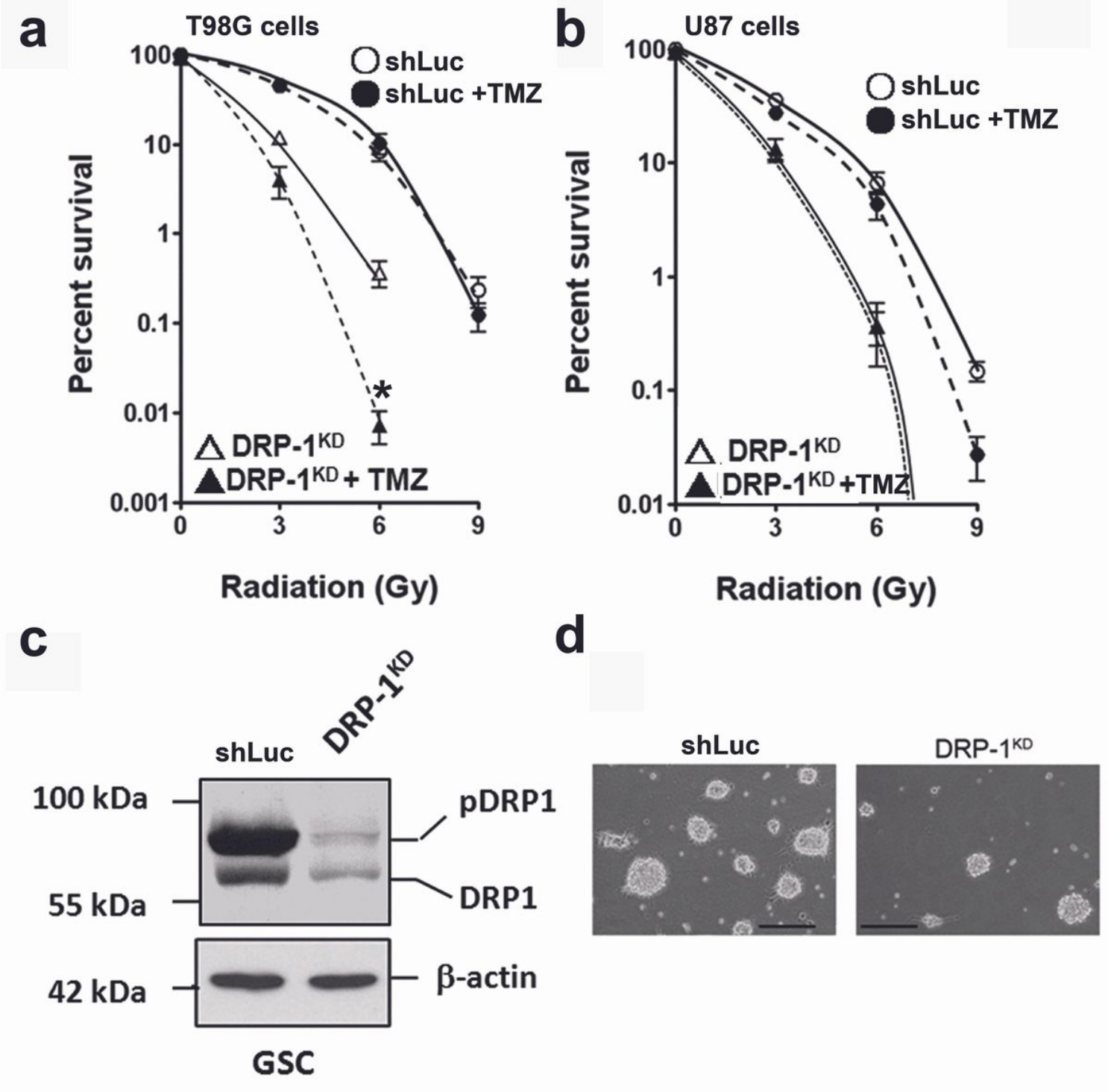

Figure 3

Correlation of DRP1 expression with radiation sensitivity of GBM and proliferation efficiency of GBM stem cells. (A) The silencing of DRP1 (DRP1KD) increased radiation-induced cell death (as measured by colony formation assay) in T98G cells. The addition of 50 M TMZ did not affect radiation resistance in wild-type ( ), but increased radiosensitivity of DRP1KD ( ) T98G cells. , wild-type; , DRP1KD cells. (B) The silencing of DRP1 (DRP1KD) also increased radiosensitivity in U87MG cells. , wild-type; , DRP1KD.

TMZ reduced radiation resistance in wild-type U87MG (□), but not evidently in DRP1KD (□) cells. MGMT promoter in U87 is methylated, and that in T98G is unmethylated. Results are the means ± S.D. of three independent experiments. *, p <0.005 (C) GBM stem cells highly expressed DRP1. The silencing of DRP1 expression (DRP1KD) reduced the DRP1 protein level (as detected by Western blotting). (D) DRP1KD GBM stem cells had lower proliferation ability (as measured by the formation of spheres). Scale bars are 250 □m. The results were repeated over three independent experiments in each case.

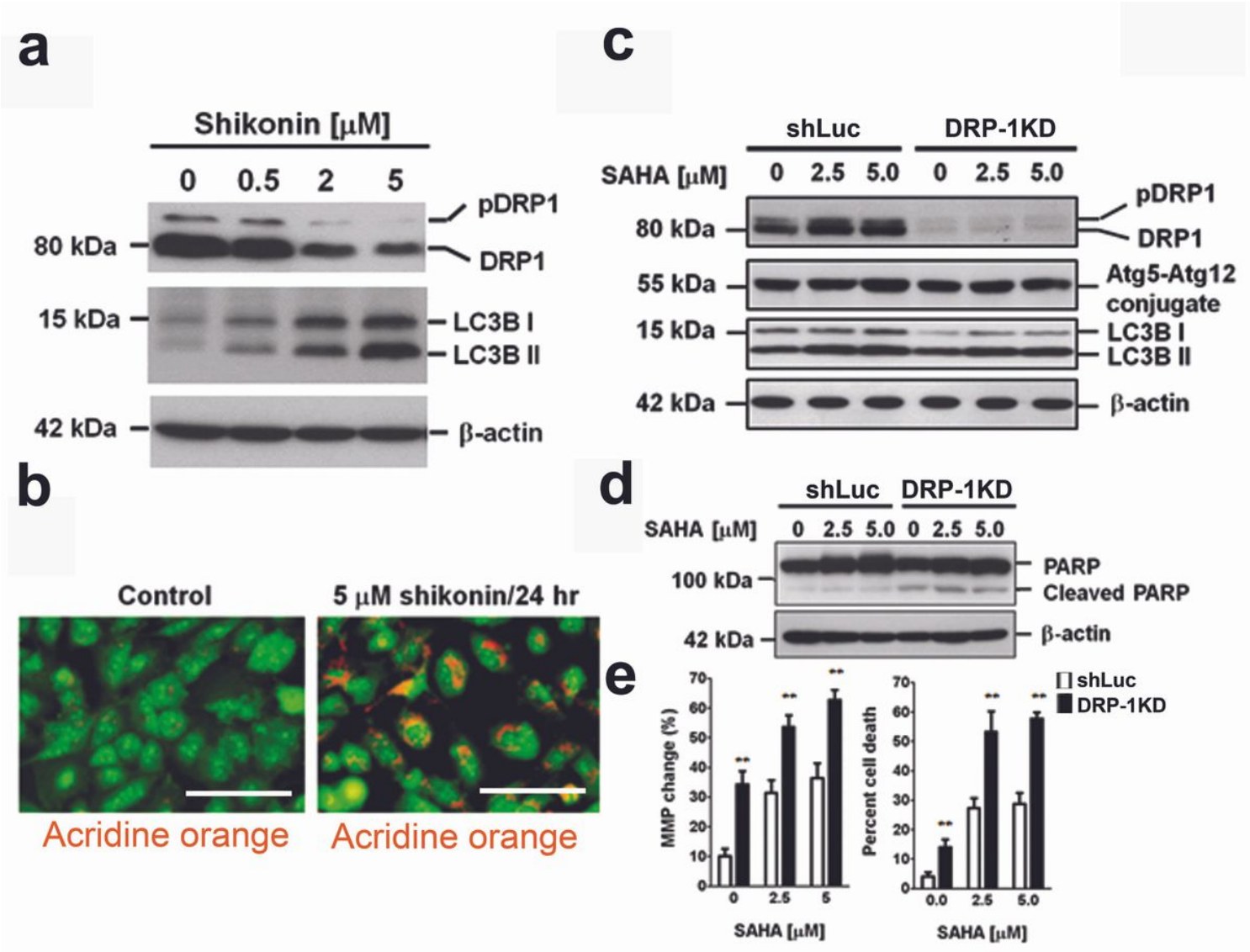

Figure 4

Shikonin and SAHA had different effects on gene expression of DRP1 in T98G cells. (A) The addition of shikonin inhibited expression of DRP1, and induced autophagy (as shown by increased levels of LC3B-II by Western blotting). (B) Treatment with shikonin for 24 hr induced autophagy, as confirmed by the formation of autophagosomes, which was visualized by using fluorescence microscopy to detect the colour change of acridine orange (change from colorless to yellow or orange under low pH). Scale bars are 100 □m. (C) The addition of SAHA did not clearly affect DRP1 expression or induce autophagy (no obvious change of autophagy markers, ATg5-Atg12 conjugates and LC3B II, was detected by Western

blotting). (D) Treatment with SAHA for 24 hr did not readily induce cleavage of poly [ADP-ribose] polymerase 1 (PARP-1), a marker of apoptosis, but clearly increase PARP-1 levels (left side). In DRP1KD T98G cells, SAHA increased PARP-1 cleavage (right side). Expression of β-actin was used as a monitoring standard for relative protein expression in the Western blotting analysis. (E) Cell death, which was measured by colony formation assay, was presented in the right panel. Changes of mitochondrial membrane potential (MMP), an indication of mitochondria depolarization, was shown in the left panel. Briefly, following SAHA treatment, T98G cells were incubated with hydrophobic fluorescent dye 3,3'-dihexyloxacarbocyanine iodide (DiOC6) at 37°C for 20 min prior to harvest. The collected cells were analyzed by the FACS Calibur (BD, CA, USA). Results are the means ± S.D. of three independent experiments. **, $p < 0.001$

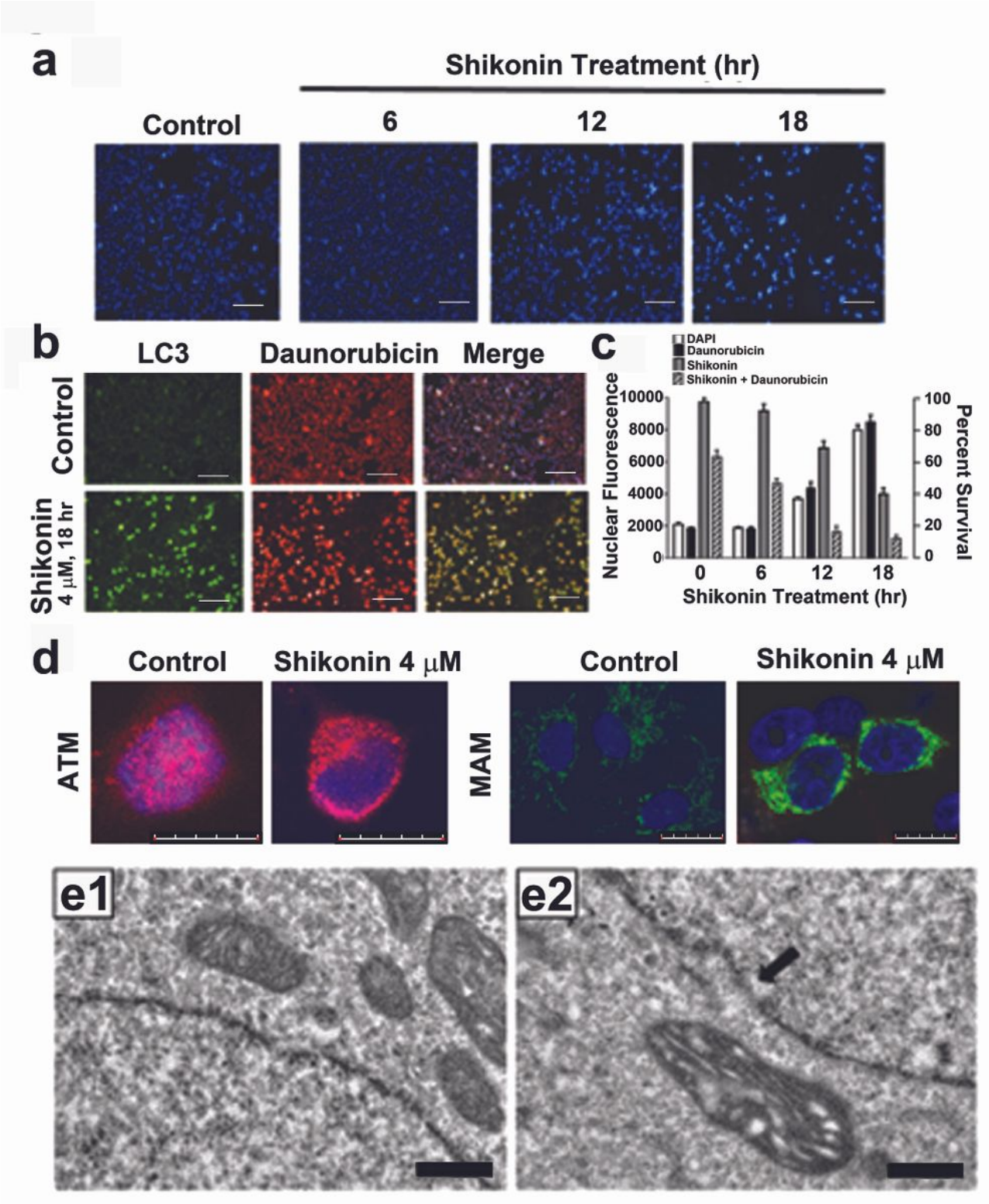

Figure 5

Shikonin increases nuclear levels of DAPI stain and anticancer drug, daunorubicin, but inhibits nuclear transportation of DNA repair-related protein, ATM. (A) 18-hr post-shikonin treatment, nuclear fluorescence of DAPI stain increased about 4 folds when T98G cells were scanned by an Operatta® imaging system. Scale bars are 250 □m. (B) Shikonin increased expression of LC3, an autophagy marker, in T98G cells. The LC3 signals were overlapped with the fluorescence of anticancer drug daunorubicin when cells were

scanned by Operatta® imaging system. Scale bars are 250 □m. (C) A schematic composite of shikonin-treated cells. White column, cells stained with DAPI (as fluorescence control); Black column, nuclear levels of daunorubicin; Grey column, cytotoxicity to shikonin alone; Slash-line column, cytotoxicity to shikonin and 0.5 □M daunorubicin, as measured by a WST-1 assay. The results were repeated over three independent experiments in each case. (D) Shikonin inhibited the nuclear transportation of ATM (red fluorescence), and the proteins were accumulated in the enlarged MAM (green fluorescence), indicating that decreasing expression of DRP1 also reduced nuclear import of DNA repair-related proteins (You et al, 2013). Scale bars are 20 □m. The above results were repeated over three independent experiments in each case. (E) Comparing to the control T98G cells (E1), shikonin induced damage of the nuclear envelops (E2, arrow) when the cells were examined by a transmission electron microscopy. Scale bars are 2.5 □m.